Transplantation of exogenous mitochondria mitigates myocardial dysfunction after cardiac arrest

Zhen Wang [1]†, Jie Zhu [1]†, Mengda Xu [2], Xuyuan Ma [3], Maozheng Shen [3], Jingyu Yan,[2] Guosheng Gan[1, 2, *], Xiang Zhou [1, 2, *]

1. The First School of Clinical Medicine, Southern Medical University, Guangzhou, China
2. Department of Anesthesiology, General hospital of central theater command of PLA, Wuhan, China
3. Base of Central Theater Command of People's Liberation Army, Hubei University of Medicine, Wuhan, China

[*] Corresponding author to Guosheng Gan(526193186@qq.com), and Xiang Zhou(zhouxiang188483@126.com)

†These authors contributed equally to this work and should be considered as co-first authors

Abstract The incidence of post-cardiac arrest myocardial dysfunction (PAMD) is high, and there is currently no effective treatment available. This study aims to investigate the protective effects of exogenous mitochondrial transplantation. Exogenous mitochondrial transplantation can enhance myocardial function and improve the survival rate. Mechanistic studies suggest that mitochondrial transplantation can limit impairment in mitochondrial morphology, augment the activity of mitochondrial complexes II and IV, and raise ATP levels. As well, mitochondrial therapy ameliorated oxidative stress imbalance, reduced myocardial injury, and thus improved PAMD after cardiopulmonary resuscitation (CPR).

Keywords: mitochondrial transplantation; cardiac arrest; post-cardiopulmonary resuscitation myocardial dysfunction; cardioprotection; ischemia

Introduction

Cardiac arrest (CA) is a life-threatening event that is followed by post-cardiac arrest myocardial dysfunction (PAMD) after the return of spontaneous circulation (ROSC). PAMD exhibits degrees of systolic and diastolic dysfunction. The heart requires up to 30 kg of ATP daily to maintain systolic function (***Hall, et al.**,**2014***). Due to the high energy requirements of the myocardium, mitochondria make up approximately one-third of the volume of cardiomyocytes (***Cao, et al.,2023***). The occurrence of PAMD is associated with mitochondrial damage with increased mitochondrial volume, accumulation of calcium ions, a diminution in complex activity, and a decrease in phosphate synthesis (***Huang, et al.**,**2015***; ***McCully, et al.**,**2023***; ***Su, et al.**,**2021***; ***Tsai, et al.**,**2021***). Myocardium, as a high energy-consuming tissue, is very susceptible to energy depletion due to mitochondrial dysfunction. After mitochondrial injury, cytoplasmic and mitochondrial calcium overload prevents full relaxation of cardiomyocytes and can release cytochrome C to activate mitochondrial apoptotic pathways. This process contributes to the development of PAMD (***Gazmuri and***

Radhakrishnan**,**2012; ***Su, et al.**,**2021***). Therefore, maintaining cardiomyocyte mitochondrial function after cardiopulmonary resuscitation (CPR) could be useful for cell survival and tissue homeostasis.

Transplantation of mitochondria isolated from non-ischemic or allogeneic tissues promoted myocardial recovery after regional ischemia (***McCully, et al.**,**2009***). Although the safety and efficacy of this approach have been verified (***Ali, et al.**,**2021***; ***Jia, et al.**,**2022***), effectiveness of mitochondrial transplantation in treating myocardial injury following cardiac arrest remains to be demonstrated. Herein, we performed mitochondrial transplantation in rats following CPR to observe its effects on cardiac function and prognosis and explored its potential mechanism of action.

Results

CA-CPR model

No significant differences in weight or temperature were found between any groups before modeling. There was no significant difference in CA induction or CPR duration among the NS, Vehicle, and Mito groups. Compared to the Sham group, the other three groups tended to receive less anesthetic (Table 1).

Mitochondrial transplantation improves cardiac function and does not alter hemodynamics in rats.

Echocardiography revealed no differences in cardiac function among the groups prior to CA-CPR. Compared to the baseline, the left ventricular ejection fraction of rats subjected to CA-CPR significantly decreased after ROSC at 1 hour, and gradually improved over time ($P<0.05$; Fig. 2A, 2B). Of note, the level of cardiac-function impairment in the Mito group was significantly reduced four hours after ROSC compared to the NS and Vehicle groups ($P<0.05$).

Compared to the Sham group, the mean arterial pressure (MAP) and heart rate (HR) of the other groups decreased at 1, 2, 3, and 4 hours after ROSC, reaching their nadir at 1 hour. MAP and HR then increased gradually but remained lower than in the Sham group at four hours. MAP and HR did not differ at any observational timepoints ($P>0.05$, Fig. 2C).

Mitochondrial transplantation improves the 72-h survival rate after cardiopulmonary resuscitation in rats.

In animals not treated with mitochondria, Kaplan-Meier analysis found a rapid drop in the survival rate of rats within 24 hours after ROSC. In contrast, the survival rate of the Mito group was significantly higher than that of the NS and Vehicle groups ($P<0.05$, Fig.2D).

Viability and purity of isolated mitochondria

Under conditions of elevated mitochondrial membrane potential, JC-1 was noted to aggregate and produced red fluorescence. Nearly all of the mitochondria isolated from healthy rats a high membrane potential, suggesting more viability (Fig. 3A). Mitochondria purity was confirmed by immunoblotting for COX-IV (a mitochondrial-specific protein) in both skeletal samples and isolated mitochondrial proteins. GAPDH was only detected in skeletal muscle proteins (Fig. 3B).

Effects of mitochondrial transplantation on cardiomyocyte mitochondria

Transplanted Mitochondria are internalized by cardiomyocytes. Animals received mitochondria pre-labeled with MitoTracker Red CMXRos. Four hours after injection, analysis of tissue sections found labelled mitochondria in epicardium, muscle, and endocardium (Fig. 4A).

Mitochondrial transplantation does not alter the mass of myocardial mitochondria. To investigate the potential increase in mitochondrial mass in myocardial cells through mitochondrial transplantation, the expression of TOM20 (a commonly used marker for mitochondrial mass) was assessed in each group using tissue immunofluorescence staining. After four hours of ROSC, there was no significant difference in the TOM20 level (as reflected by fluorescence intensity) among the groups, suggesting that mitochondrial transplantation did not increase the mass of mitochondria in the hearts. (Figures 4E, 4F).

Mitochondrial transplantation improves cardiac mitochondrial structure. In the NS and Vehicle groups, the myocardial myofibrils exhibited a disordered arrangement on EM, with variation in sarcomeres length and loss of Z-lines. Translucent and swollen mitochondria were visible, exhibiting a larger gap between membranes, distorted cristae, and accumulated calcium. In contrast, the mitochondria sarcomeres of the Mito group were more distinct, and the myocardial myofibrils were arranged in a more orderly fashion. The M-lines and Z-lines were clearly visible, and the number of mitochondrial cristae had increased, with their structure appearing to be complete (Fig. 4G).

Mitochondrial transplantation improves mitochondrial metabolism of cardiac tissue after CA-CPR. The activity of mitochondrial complexes II and IV and ATP content in cardiac tissue was characterized. Compared to the Sham group, complex II and IV activity and ATP content were significantly attenuated in the other groups ($P<0.05$). In contrast, the activities of complexes II and IV and ATP content were significantly elevated in the Mito group compared to the NS and Vehicle groups, suggesting that transfer of exogenous mitochondria enhanced function and energy metabolism or resident mitochondria ($P<0.05$, Fig. 4B, 4C, 4D).

Effects of mitochondrial transplantation on cardiomyocytes

Mitochondrial transplantation alleviates myocardial oxidative stress injury after CA-CPR. MDA levels in the myocardial tissue of rats four hours after ROSC was decreased in animals given exogenous mitochondria CPR ($P<0.05$) (Fig. 5A). Additionally, the activity of SOD was significantly increased in the Mito group relative to the NS and Vehicle groups ($P<0.05$).

Mitochondrial transplantation reduces cardiomyocyte apoptosis. Apoptotic indices and apoptotic rate as assessed by flow cytometry increased four hours after ROSC. Compared with the NS and Vehicle groups, the apoptotic index and apoptotic rate by in the Mito group were lower ($P<0.05$). This links exogenous mitochondrial transplantation to reduced cardiomyocyte apoptosis after CPR (Fig. 5B, 5C, 5D).

Mitochondrial transplantation reduces the markers of myocardial injury. ELISA was used to detect the expression of myocardial injury markers, CK-MB and cTn-I, at four hours of ROSC. Compared to the Sham group, the levels of CK-MB and cTn-I in the serum of the other groups showed a significant rise ($P<0.05$). However, both CK-MB and cTn-I levels in the serum of the Mito group were lower than those in the NS and Vehicle groups, suggesting that myocardial injury was reduced ($P<0.05$, Fig. 5F).

Mitochondrial transplantation attenuates myocardial histopathologic changes. Four hours of ROSC, Tissue samples from sham group exhibited a well-organized structure of myocardial fibers, with no apparent inflammatory cell infiltration into the stroma (Fig.5E). In the NS and Vehicle groups, the myocardial fibers were disordered, with some myocardial cells exhibiting thickening, rupture, and vacuolization. Also, there was noticeable inflammatory cell invasion of the stroma. The myocardial arrangement in the Mito group was more neatly arranged than that in the NS and Vehicle groups although thickening of myocardial cells was noted.

Discussion

PRMD is a common complication following resuscitated. It is characterized by systolic and diastolic insufficiency, arrhythmias, and recurrent cardiac arrest. Circulatory dysfunction occurs in approximately two-thirds of cardiac arrest subjects is associated with a poor outcome (***Han and Lee**,**2022***). Unlike myocardial depression caused by regional ischemia characterized by localized ventricular wall-motion abnormalities, myocardial depression caused by PAMD after CA manifest as global left ventricular systolic dysfunction accompanied by reduced ejection fraction, left ventricular diastolic dysfunction, and right ventricular dysfunction (***Lazzarin, et al.**,**2022***; ***Xu, et al.**,**2008***). Of these, global left ventricular systolic dysfunction is the most significant manifestation.

In the present study, we test the hypothesis that administration of exogenous mitochondrial is cardioprotective effects after cardiopulmonary resuscitation. The rationale was to enhance the energy-dependent contractility of the myocardium. Mitochondria from non-ischemic gastrocnemius muscle of health donor animals were isolated and a manner that maximized their healing potential. Of import, uptake of the delivered mitochondria occurred in the heart and myocytes, perhaps via micropinocytosis (Fig. 6) (***Kami and Gojo**,**2020***). AS well, mitochondrial internalization occurred through actin-dependent endocytosis (***Pacak, et al.**,**2015***). Internalized mitochondria promote degradation of resident via lysosomes to maintain an energy mitochondrial balance (***Jia, et al.**,**2022***; ***Liu, et al.**,**2022***). Internalized mitochondria facilitated respiratory restoration in recipient cells with depleted mtDNA, and improved cellular function by increasing ATP levels and oxygen-consumption rates (***Pacak, et al.**,**2015***).

Contrary to expectations, increased numbers of mitochondria were not found in the hearts of treated animals. Possibly CPR caused ischemia/reperfusion injury to organs throughout the body, with non-specific distribution and uptake of the delivered mitochondria. The results of our study are consistent with other date that the energy metabolism of myocardial mitochondria improved after mitochondrial transplantation along with increased complex activity and ATP content (***Jia, et al.**,**2022***; ***Pacak, et al.**,**2015***). Not surprisingly, mitochondrial transplantation is being pursued as a therapeutic strategy in part to effects coronary patency, autoimmunity, and arrhythmia attacks (***Masuzawa, et al.**,**2013***; ***Shin, et al.**,**2019***). The clinical application of mitochondrial transplantation can enhance the prognosis of pediatric patients requiring extracorporeal membrane oxygenation following cardiac surgery, the improvement of cardiac function in patients helps them successfully wean off ECMO support (***Emani and McCully**,**2018***). It is worth noting that the method of mitochondrial isolation may better meet the needs of clinical settings where an interventional time below 60 min is desired (***Ali, et al.**,**2021***). After the isolation, mitochondria can be immediately used for transfer and internalization (***Ali, et al.**,**2021***). Still concerns regarding mitochondrial hemocompatibility and stability in serum have been raised. In this line, serum calcium did not adversely impact isolated mitochondria (***Maleki, et al.**,**2023***).

ROS is generated with ischemia and then targets the normal physiologic functions of cells by damaging the structures of proteins, lipids, and even DNA (***Zhu, et al.**,**2024***). As well, oxidative stress promotes cardiac ischemia-reperfusion injury and was implicated in pro-inflammatory responses and apoptosis, both of which worsen myocardial cell injury (***Patel and Karch**,**2020***). In a regional ischemia-reperfusion model, mitochondrial transplantation reduced oxidative stress in cells following reperfusion (***Zhang, et al.**,**2019***). Similaerly, in the present study, mitochondrial transplantation decreased the levels of myocardial oxidative markers and increased the expression of antioxidant enzymes after four hours of ROSC.

Ischemia/reperfusion injury of myocardial tissue releases CK-MB and cTn-I, commonly used indicators of early myocardial injury in clinical settings (***Zhang, et al.**,**2021***). Although the concentrations of CK-MB and cTn-I rose significantly four hours after resuscitation in the CA-CPR model, mitochondrial transplantation significantly reduced this effect. During ischemia, the loss of mitochondrial membrane potential leads to mitochondrial swelling and the release of cytochrome C followed by caspase-mediated cell death during reperfusion (***Lu, et al.**,**2023***; ***Milliken, et al.**,**2022***). Apoptosis is the process by which cardiomyocytes die (***Kunapuli, et al.**,**2006***). Increase apoptosis was found in rats after CA-CPR along with increased caspase-3 expression after resuscitation (***Wu, et al.**,**2021***). Similar results were reported in pigs that underwent CA-CPR (***Wang, et al.**,**2023***). We found that the level of apoptosis in cardiomyocytes increased significantly after CPR whereas administration of healthy mitochondria significantly reduced cardiomyocyte apoptosis.

Exogenous mitochondrial transplantation significantly reduced the disordering of myocardial fiber arrangement and inflammatory cell infiltration.

In conclusion, exogenous mitochondrial transplantation improved cardiac function after CPR. The specific mechanism involved may be related to the improvement in mitochondrial function, thus reducing the oxidative-stress response and apoptosis of myocardial cells. These dates suggest possible advantage in mitochondrial transplantation following cardiopulmonary resuscitation.

Limitations

Hemodynamic observation was carried out only for four hours after cardiopulmonary resuscitation, Thus, the impact of mitochondrial transplantation on long-term cardiac function following cardiopulmonary resuscitation could not be assessed. In this study, the animal model consisted of healthy rats. However, in clinical practice, CA is primarily caused by cardiac issues. Healthy rats tend to exhibit higher recovery ability after CA, which may lead to an overestimation of the therapeutic effects of mitochondrial transplantation. In our next phase, we plan to utilize various cardiac arrest models in conducting comprehensive studies to validate the effectiveness of mitochondrial transplantation in different pathological models.

Methods

Animals

The experimental protocol (Fig.1) was approved by the Animal Experiment Committee of the General Hospital of Central Theater Command (No.2023017) and conformed to the Guide for the Care and Use of Experimental Animals published by the National Institutes of Health, USA (NIH Publication No. 5377-3, 1996). Adult male SD (7 to 8 weeks old) rats weighing 250 to 350g were purchased from Hunan Silaidajing Experimental Animal Co., Ltd. (No. 430727231102711675, Changsha, China). Male rats were selected to avoid estrous cycle interference. Animals were housed in standard cages with a 12-hour light-dark cycle at a room temperature 22°C.

Animals were randomly assigned to four groups using the random number table method: a sham group, NS group, Vehicle group, and Mito group (n=17 per group). Each group was further divided into two survival-analysis subgroups: a four-hour group (n=7) and a 72-hour group (n=10). Rats in the NS, Vehicle and Mito groups underwent cardiac arrest induced by asphyxia and CPR, while rats in the sham group underwent tracheal intubation and arteriovenous puncture only, without CA and CPR.

Experimental protocol

CA-CPR model Establishment of the CA-CPR model was as published previous (***Huang, et al.**,**2020***). Rats were anesthetized with pentobarbital sodium (45 mg/kg) i.p. A 16-G intravenous catheter was used for endotracheal intubation. The left femoral artery and the right femoral vein were subsequently connected using a 24-G venous indwelling needle for dynamic blood pressure detection and venous-access establishment. Blood pressure, heart rate, and rectal temperature were monitored using the ALC-MPA monitoring system (Alcott Biotech, Shanghai, China). After 10 minutes of mechanical ventilation, asphyxia-mediated cardiac arrest was induced by blocking the tracheal tube. CA was defined as a decrease in systolic blood pressure to 25 mmHg. Five minutes after CA, external chest compression (200 bpm) and mechanical ventilation (tidal volume, 0.60 ml/100 g, respiratory rate, 80 bpm) were initiated, and epinephrine (40 mcg/kg) was administered intravenously. Return of spontaneous circulation (ROSC) was defined as the spontaneous restoration of sinus rhythm with a systolic blood pressure of >60 mmHg that was maintained for 10 minutes. Subsequently, corresponding treatments were administered. Animals that did not regain autonomic circulation within five minutes were excluded from the study. After ROSC, hemodynamics and echocardiograms were recorded for 4 hours. Basal body temperature was maintained at 37°C throughout the intervention. Pentobarbital sodium (10 mg/kg) was given if animals urinated or showed increased limb-muscle tension. Twenty-eight animals of four-hour group completed the full protocol and were humanely euthanized with excess pentobarbital sodium 4 hours after ROSC. Myocardial tissue and blood samples were collected for detection. The remaining 40 animals of 72-hour group were monitored for 72-hour to track survival.

Intervention measures Ten minutes after ROSC, 0.5 ml of saline, 0.5 ml of respiration buffer, and 0.5 ml of 1×10^{9}/mL mitochondrial suspension were injected through the femoral vein in the NS, Vehicle, and Mito groups, The Sham group received 0.5 ml of saline at 30 minutes postoperatively.

Echocardiography

To assess myocardial function, an ultra-high resolution, small-animal ultrasound imaging system (SigmaVET, Esaote, Genoa, Italy) was used to capture M-mode echocardiographic images at the parasternal long axis and/or parasternal short axis near the papillary muscle at 1-, 2-, 3-, and 4-hours post-ROSC.

Survival analysis

In the 72-hour survival study cohort, the catheters were extracted four hours post-ROSC, and the surgical incisions were closed. Animals were placed back in their cages and administered subcutaneous injections of 0.5ml of 1% lidocaine for analgesia. Animals were monitored every 2 hours during the initial 24 hours following ROSC, and then at 48 and 72 hours. Animals that exhibited signs such as wheezing or a respiratory rate below five breaths per minute were deemed moribund and humanely euthanized (***Su, et al.**,**2021***). At the end of the time rats were euthanized.

Isolation and identification of mitochondria

Mitochondrial isolation and labeling. Mitochondria were isolated as published.[31] In brief, 180 mg of gastrocnemius muscle obtained from healthy rats was placed into a centrifuge tube containing 5 ml of pre-chilled homogenizing buffer (300 mM sucrose, 10 mM K-HEPES, and 1 mM K-EGTA), homogenized, and incubated on ice with *Bacillus subtilis* A protease (P5380, Sigma Aldrich, Darmstadt, Germany) for 10 minutes. The mixture was filtered through a 40-μm cell filter, bovine serum albumin (ST023-50 g, Beyotime, Shanghai, China) was added and incubated for five minutes. The homogenate was then filtered through a 40-um screen and then through a 10-um screen, and centrifuged at 9000 g for 10 minutes at 4℃. The precipitate was reconstituted in 1 ml of pre-chilled respiration buffer (250 mM sucrose, 2 mM potassium dihydrogen phosphate, 10 mM magnesium chloride, 20 mM K-HEPES, and 0.5 mM K-EGTA). Mitochondrial counts were as previously published and were quantified using a fluorescence microscope (BX53, OLYMPUS, Tokyo, Japan) (***McCully, et al.***,***2009***). The isolated mitochondria were incubated with MitoTracker Red CMXRos (C1049B-50ug, Beyotime, Shanghai, China) and washed with respiratory buffer prior to administration.

Detection of mitochondrial membrane potential. A mitochondrial membrane potential detection kit (JC-1) (C2003S; Beyotime, Shanghai, China) was used to characterize function. Purified mitochondria were incubated with JC-1 staining solution at 4℃ for a duration of 60 minutes followed by imaging using a fluorescence microscope.

Western blotting. Total protein was extracted from skeletal muscle and purified mitochondria. Protein concentration was determined by the BCA method. Protein was boiled in a water bath for 10 minutes. Electrophoresis was performed using a 12% SDS-PAGE gel (P0012A, Beyotime, Shanghai, China), followed by transfer to a PVDF membrane (FFP70, Beyotime, Shanghai, China). Non-specific binding was blocked with 5% skim milk powder at room temperature for two hours. Membranes were exposed to primary antibodies overnight at 4℃: COX -IV (1:1000; AC610, Beyotime, Shanghai, China) and GAPDH (1:3000; LF206, Epizyme, Shanghai, China) on a shaker at 4℃ for 12 hours. After washing, membranes were incubated with horseradish peroxidase-labeled secondary antibody for two hours and developed with the ECL chemiluminescence method.

Mitochondrial distribution and uptake

Mitochondrial co-localization was determined as published (***Masuzawa, et al.***,***2013***). Tissue sections were incubated with 0.25% Triton-X-100 for 10 minutes at room temperature, blocked with normal bovine serum albumin, and incubated with primary antibody generated against alpha-actinin 2 (1:500; GTX103219; GeneTex, Irvine, USA) at 4℃ overnight. After washing with PBST, sections were incubated with an Alexa Fluor 488-labeled secondary antibody (1:1000, HZ0176; Huzhen, Shanghai, China) for one hour. DAPI (P0131-5 ml; Beyotime, Shanghai, China) was applied to stain nuclei. Images were acquired using the Olympus fluorescence microscope.

Analysis of cardiac mitochondria

Complex activity. Mitochondria were extracted from 0.1 g of myocardial tissue using differential centrifugation. The mitochondrial suspension was disrupted by ultrasonic waves in an ice bath releasing the mitochondrial respiratory chain complex. The working solution from mitochondrial complex activity test kit (AKOP008M, AKOP006M; Boxbio, Beijing, China) was mixed with the samples and the absorbance at 605 nm and 550 nm measured values at various timepoints. The variance between the two timepoints was calculated and recorded as ΔA1 and ΔA2. Protein concentration (C) of each sample was measured. Mitochondrial complex II activity was calculated as 476.19 × ΔA1/C, and mitochondrial complex IV activity was calculated as 1099.48 × ΔA2/C.

ATP determination. ATP levels were determined using an ATP-content test kit (A095-1-1; Nanjing Jiancheng, Nanjing, China).

Tom20 labeling. Tissue sections were labeled with Tom20 antibody (1:100, AF5206; Affinity, Changzhou, China), incubated with a horseradish peroxidase-coupled secondary antibody (1:400, 5220-0336; SeraCare, Massachusetts, USA), subjected to tyramide signal amplification (TSA), stained with DAPI and images acquired using an Olympus fluorescence microscope.

Transmission electron microscope. Fixed hearts were rinsed with phosphate-buffered saline (PBS) for 45 minutes and exposed to 1% osmium tetroxide for two hours. After dehydration in graded ethanol concentrations, tissue samples were immersed in epoxy resin, embedded, and cut into ultrathin sections (60-80 nm). The sections were stained with uranium and lead, and examined and imaged using a transmission electron microscope (HT7800; Hitachi, Tokyo, Japan).

Quantification of MDA and SOD detection. The SOD activity and MDA levels of myocardial samples were determined with a malondialdehyde (MDA) test kit (A003-1; Nanjing Jiancheng, Nanjing, China) and superoxide dismutase (SOD) test kit (A001-3; Nanjing Jiancheng, Nanjing, China).

Detection of myocardial injury

TUNEL assay. Paraffin-embedded tissue sections were processed with an *in-situ* cell-death detection kit (11684795910; Roche, Basel, Switzerland) for terminal deoxynucleotidyl transferase-mediated deoxyuridine triphosphate nick-end labeling. The ratio of TUNEL-positive cells to total cells was determined.

Flow cytometry. To prepare a single-cell suspension, myocardium tissue samples were digested with collagenase II at 37°C and filtered. Cells were washed with PBS, suspended in the binding buffer and stained with Annexin-V (Annexin-V PI cell double-staining apoptosis-detection kit; A211-02; Vazyme, Nanjing, China). Apoptosis was assessed using flow cytometry.

Markers of ischemic injury. Blood from rats was obtained the femoral artery and the serum separated. The levels of myocardial-injury markers were measured using the Creatine Kinase MB isoenzyme (CK-MB) kit (MM-0625R1; Meimian, Yancheng, China) and the Cardiac Troponin I (cTn-I) kit (MM-0426R2; Meimian, Yancheng, China).

Histology. Hearts was fixed in 4% paraformaldehyde for 24 hours, dehydrated, rendered transparent, embedded in paraffin and cut into thin sections. After dewaxing and rehydration, the sections were stained with hematoxylin and eosin, and images acquired using a light microscope.

Statistics and data analysis

IBM SPSS Statistics software (V26.0, IBM Corp, New York, USA) was used for data analysis. All data are expressed as mean ± standard deviation (Mean ± SD). Sample size for the four-hour group was calculated as published (***Dell, et al.***,***2002***). The ejection fraction of the first three surviving rats among the groups was measured. The population standard deviation of the variable is 11.34. With a magnitude of difference set at 15, an error rate of 0.1, and a power of 80%, the smallest acceptable sample size was determined to be five animals. Considering an animal loss of approximately 20% after four hours of CPR, seven animals were selected for each group. The sample size for the 72-hour group was calculated using StatBox (StatBox-Open 0.1.0; Cloud Powered Clinical Trial, Hebei, China). Set the survival rate at 20% for survival rate 1 and 80% for survival rate 2 (with power = 0.8 and $\alpha = 0.05$). Accordingly, 10 was the smallest acceptable animal sample size. The comparison of time-based measurements was evaluated using repeated-measures tow-way ANOVA, with groups as the between-subjects factor and time as the within-subjects factor. One-way ANOVA and Tukey's multiple-comparison test were employed to compare multiple groups.

Survival was characterized using the Kaplan-Meier survival analysis test. Statistical significance was defined at $P<0.05$.

Acknowledgments

We thank LetPub (www.letpub.com) for linguistic assistance and pre-submission expert review.

Additional information

Funding

This work was supported by the National Natural Science Foundation of China (82372210, 81901932) and Natural Science Foundation of Hubei Province (2021CFB492).

Author contributions

X.Z. and G.S.G. supervised the study and designed the experiments. Z.W. and J.Z performed the experiments. Z.W and J.Z. collected, analyzed and interpreted the data. M.D.X. and J.Y.Y. supervised the experiments. X.Y.M. and M.Z.S. accessed and verified the data. Z.W. and J.Z. wrote the manuscript. X.Z. and G.S.G. revised the manuscript. All authors read and approved the final version of the manuscript.

Ethics

The animal experiments were approved by the Animal Experiment Committee of the General Hospital of Central Theater Command (No.2023017).

Additional files

Supplementary files

Supplementary file 1. Details of antibodies used in the methodology

Data availability

The data underlying this article will be shared on reasonable request to the corresponding author.

References

Ali PP, Hosseinian S, Kheradvar A. 2021. Mitochondrial transplantation in cardiomyocytes: foundation, methods, and outcomes. *American Journal of Physiology-Cell Physiology* **321**:C489-C503. DOI:10.1152/ajpcell.00152.2021, PIMD: 34191626.

Cao X, Yao F, Zhang B, Sun X. 2023. Mitochondrial dysfunction in heart diseases: Potential therapeutic effects of Panax ginseng. *Frontiers in Pharmacology* **14**:1218803. DOI:10.3389/fphar.2023.1218803, PIMD:37547332.

Dell RB, Holleran S, Ramakrishnan R. 2002. Sample size determination. *Ilar Journal* **43**:207-213. DOI:10.1093/ilar.43.4.207, PIMD: 12391396.

Emani SM, McCully JD. 2018. Mitochondrial transplantation: applications for pediatric patients with congenital heart disease. *Translational Pediatrics* **7**:169-175. DOI:10.21037/tp.2018.02.02, PIMD: 29770298.

Gazmuri RJ, Radhakrishnan J. 2012. Protecting mitochondrial bioenergetic function during resuscitation from cardiac arrest. *Critical Care Clinics* **28**:245-270.

DOI:10.1016/j.ccc.2012.02.001, PIMD: 22433486.

Hall AR, Burke N, Dongworth RK, Hausenloy DJ. 2014. Mitochondrial fusion and fission proteins: novel therapeutic targets for combating cardiovascular disease. *British Journal of Pharmacology* **171**:1890-1906. DOI:10.1111/bph.12516, PIMD: 24328763.

Han C, Lee JH. 2022. Heart rate and diastolic arterial pressure in cardiac arrest patients: A nationwide, multicenter prospective registry. *Public Library of Science ONE* **17**: e274130. DOI:10.1371/journal.pone.0274130, PIMD: 36103505.

Huang CH, Tsai MS, Chiang CY, Su YJ, Wang TD, Chang WT, Chen HW, Chen WJ. 2015. Activation of mitochondrial STAT-3 and reduced mitochondria damage during hypothermia treatment for post-cardiac arrest myocardial dysfunction. *Basic Research in Cardiology* **110**:59. DOI:10.1007/s00395-015-0516-3, PIMD: 26471891.

Huang Y, Gao X, Zhou X, Xie B, Zhang Y, Zhu J, Zhu S. 2020. Mitophagy in the Hippocampus Is Excessive Activated After Cardiac Arrest and Cardiopulmonary Resuscitation. *Neurochemical Research* **45**:322-330. DOI:10.1007/s11064-019-02916-z, PIMD: 31773373.

Jia L, Yang L, Tian Y, Yang L, Wu D, Zhang H, Li M, Wu N. 2022. Nrf2 participates in the protective effect of exogenous mitochondria against mitochondrial dysfunction in myocardial ischaemic and hypoxic injury. *Cellular Signalling* **92**:110266. DOI:10.1016/j.cellsig.2022.110266, PIMD: 35091043.

Kami D, Gojo S. 2020. From Cell Entry to Engraftment of Exogenous Mitochondria. *International Journal of Molecular Sciences* **21.** DOI:10.3390/ijms21144995, PIMD: 32679802.

Kunapuli S, Rosanio S, Schwarz ER. 2006. "How do cardiomyocytes die?" apoptosis and autophagic cell death in cardiac myocytes. *Journal Of Cardiac Failure* 12:381-391. DOI:10.1016/j.cardfail.2006.02.002, PIMD: 16762802.

Lazzarin T, Tonon CR, Martins D, Fávero EJ, Baumgratz TD, Pereira F, Pinheiro VR, Ballarin RS, Queiroz D, Azevedo PS, Polegato BF, Okoshi MP, Zornoff L, Rupp DPS, Minicucci MF. 2022. Post-Cardiac Arrest: Mechanisms, Management, and Future Perspectives. Journal of Clinical Medicine **12**. DOI:10.3390/jcm12010259, PIMD:

36615059.

Liu Z, Sun Y, Qi Z, Cao L, Ding S. 2022. Mitochondrial transfer/transplantation: an emerging therapeutic approach for multiple diseases. Cell and Bioscience **12**:66. DOI:10.1186/s13578-022-00805-7, PIMD: 35590379.

Lu CH, Chen DX, Dong K, Wu YJ, Na N, Wen H, Hu YS, Liang YY, Wu SY, Lin BY, Huang F, Zeng ZY. 2023. Inhibition of miR-143-3p alleviates myocardial ischemia reperfusion injury via limiting mitochondria-mediated apoptosis. *JOURNAL OF BIOLOGICAL CHEMISTRY* **404**:619-631. DOI:10.1515/hsz-2022-0334, PIMD: 36780323.

Maleki F, Rabbani S, Shirkoohi R, Rezaei M. 2023. Allogeneic mitochondrial transplantation ameliorates cardiac dysfunction due to doxorubicin: An in vivo study. *Biomedicine & Pharmacotherapy* **168**:115651. DOI:10.1016/j.biopha.2023.115651, PIMD: 37812888.

Masuzawa A, Black KM, Pacak CA, Ericsson M, Barnett RJ, Drumm C, Seth P, Bloch DB, Levitsky S, Cowan DB, McCully JD. 2013. Transplantation of autologously derived mitochondria protects the heart from ischemia-reperfusion injury. *American Journal of Physiology-heart And Circulatory Physiology* **304**:H966-H982. DOI:10.1152/ajpheart.00883.2012, PIMD: 23355340.

McCully JD, Cowan DB, Pacak CA, Toumpoulis IK, Dayalan H, Levitsky S. 2009. Injection of isolated mitochondria during early reperfusion for cardioprotection. *American Journal of Physiology-heart And Circulatory Physiology* **296**:H94-H105. DOI:10.1152/ajpheart.00567.2008, PIMD: 18978192.

McCully JD, Del NP, Emani SM. 2023. Mitochondrial transplantation: the advance to therapeutic application and molecular modulation. *Frontiers In Cardiovascular Medicine* **10**:1268814. DOI:10.3389/fcvm.2023.1268814, PIMD: 38162128.

Milliken AS, Nadtochiy SM, Brookes PS. 2022. Inhibiting Succinate Release Worsens Cardiac Reperfusion Injury by Enhancing Mitochondrial Reactive Oxygen Species Generation. *Journal Of The American Heart Association* **11**:e26135. DOI:10.1161/JAHA.122.026135, PIMD: 35766275.

Pacak CA, Preble JM, Kondo H, Seibel P, Levitsky S, Del NP, Cowan DB, McCully

JD. 2015. Actin-dependent mitochondrial internalization in cardiomyocytes: evidence for rescue of mitochondrial function. *Biology Open* **4**:622-626. DOI:10.1242/bio.201511478, PIMD: 25862247.

Patel P, Karch J. 2020. Regulation of cell death in the cardiovascular system. *International Review of Cell and Molecular Biology* **353**:153-209. DOI:10.1016/bs.ircmb.2019.11.005, PIMD: 32381175.

Preble JM, Pacak CA, Kondo H, MacKay AA, Cowan DB, McCully JD. 2014. Rapid isolation and purification of mitochondria for transplantation by tissue dissociation and differential filtration. *Journal of Visualized Experiments* 6:e51682. DOI:10.3791/51682, PIMD: 25225817.

Shin B, Saeed MY, Esch JJ, Guariento A, Blitzer D, Moskowitzova K, Ramirez-Barbieri G, Orfany A, Thedsanamoorthy JK, Cowan DB, Inkster JA, Snay ER, Staffa SJ, Packard AB, Zurakowski D, Del NP, McCully JD. 2019. A Novel Biological Strategy for Myocardial Protection by Intracoronary Delivery of Mitochondria: Safety and Efficacy. *JACC: Basic to Translational Science* **4**:871-888. DOI:10.1016/j.jacbts.2019.08.007, PIMD: 31909298.

Su C, Fan X, Xu F, Wang J, Chen Y. 2021. Prostaglandin E1 attenuates post-cardiac arrest myocardial dysfunction through inhibition of mitochondria-mediated cardiomyocyte apoptosis. *Molecular Medicine Reports* **23** DOI:10.3892/mmr.2020.11749, PIMD: 33300050.

Tsai MS, Huang CH, Wang CH, Cheng HJ, Wu SN, Chang WT, Chen WJ. 2021. Post-Cardiac Arrest Hydrocortisone Use Ameliorates Cardiac Mitochondrial Injury in a Male Rat Model of Ventricular Fibrillation Cardiac Arrest. *Journal of the American Heart Association* **10**:e19837. DOI:10.1161/JAHA.120.019837, PIMD: 33960200.

Wang D, Wang L, Sun Y, Kong F, Jiang Y, An M, Xia Y, Gong P, Yang Y. 2023. Effects of temperature control on hyperthermia-related cardiac dysfunction in a porcine model of cardiac arrest. *Cryobiology* **110**:49-55. DOI:10.1016/j.cryobiol.2022.12.017, PIMD: 36509162.

Wu J, Chen H, Qin J, Chen N, Lu S, Jin J, Li Y. 2021. Baicalin Improves Cardiac

Outcome and Survival by Suppressing Drp1-Mediated Mitochondrial Fission after Cardiac Arrest-Induced Myocardial Damage. *Oxidative Medicine and Cellular Longevity* **2021**:8865762. DOI:10.1155/2021/8865762, PIMD: 33603953.

Xu T, Tang W, Ristagno G, Wang H, Sun S, Weil MH. 2008. Postresuscitation myocardial diastolic dysfunction following prolonged ventricular fibrillation and cardiopulmonary resuscitation. *Critical Care Medicine* **36**:188-192. DOI:10.1097/01.CCM.0000295595.72955.7C, PIMD: 18090365.

Zhang GR, Peng CM, Liu ZZ, Leng YF. 2021. The effect of dexmedetomidine on myocardial ischemia/reperfusion injury in patients undergoing cardiac surgery with cardiopulmonary bypass: a meta-analysis. *European Review for Medical and Pharmacological Sciences* **25**:7409-7417. DOI:10.26355/eurrev_202112_27438, PIMD: 34919243.

Zhang Z, Ma Z, Yan C, Pu K, Wu M, Bai J, Li Y, Wang Q. 2019. Muscle-derived autologous mitochondrial transplantation: A novel strategy for treating cerebral ischemic injury. *Behavioural Brain Research* **356**:322-331. DOI:10.1016/j.bbr.2018.09.005, PIMD: 30213662.

Zhu Y, Wang K, Jia X, Fu C, Yu H, Wang Y. 2024. Antioxidant peptides, the guardian of life from oxidative stress. *Medicinal Research Reviews* **44**:275-364. DOI:10.1002/med.21986, PIMD: 37621230.

Figure 1. Experimental design of the *in vivo* study.

Rats in all groups except the sham group underwent CA for 5 minutes and then received the corresponding intervention immediately after ROSC. ROSC was defined as the spontaneous restoration of sinus rhythm with a systolic blood pressure of >60 mmHg that was maintained for 10 minutes. Four hours after ROSC, the 4-hour group was used to collect myocardial tissue and blood samples for detection, whereas the 72-hour group was used for survival detection. BL, baseline; CA, cardiac arrest; ROSC, return of spontaneous circulation.

Figure 2. Observational results at 4 and 72 hours after cardiopulmonary resuscitation in rats.

(A) Echocardiograms of rats in each group from baseline to 4 hours following ROSC (n = 7 animals per group). (B) EF of rats in each group from baseline to 4 hours following ROSC (n = 7 animals per group). (C) HR and MAP changes during post-ROSC in 4 hours (n = 7 animals per group). (D) Survival rate during the first 72 hours following ROSC (n = 10 animals per group). Myocardial function between groups was compared by time-based measurements in each group using repeated-measures ANOVA. The survival rate between groups was compared using the Kaplan–Meier survival analysis test. * $P < 0.05$ vs. sham group and # $P < 0.05$ vs. Mito group. BL, baseline; EF, ejection fraction; HR, heart rate; MAP, mean arterial pressure; bpm, beats per minute; mmHg, millimeters of mercury; AMV, after mechanical ventilation; ROSC, return of spontaneous circulation.

Figure 3. Assessment of the viability and purity of isolated mitochondria.

(A) JC-1 staining of mitochondria after isolation from muscle. The staining of isolated mitochondria by JC-1 is visible as either red for J-aggregates or green for J-monomers. The intensity of the red color indicates that the isolated mitochondria had a high membrane potential, confirming their quality for transplantation. Scale bar = 100 μm. (B) SDS/PAGE analysis of fractions obtained during the purification of muscle mitochondria. GAPDH is only expressed in muscle, confirming its purity for transplantation.

Figure 4. Administration of mitochondria ameliorates ischemia/reperfusion–mediated mitochondrial alterations in cardiomyocytes 4 hours after ROSC.

(A) Localization and uptake of transplanted mitochondria in the heart; myocardial tissue was stained for anti-α-actinin 2 (green) and nuclei (blue); the pre-stained isolated mitochondria were labeled red (n = 3 animals per group). Scale bar = 100 μm. (B and C) Changes in myocardial mitochondrial complex II and IV enzyme activities in hearts (n = 7 animals per group). (D) The ATP content in myocardial tissue was measured via colorimetry (n = 7 animals per group). The detection of fluorescence intensity of Tom20: (E) image and (F) quantitative data. Scale bar = 100 μm (n = 3 animals per group). (G) Representative photographs of mitochondrial morphology by TEM examination; arrows indicate calcium accumulation (n = 3 animals per group). Scale bars = 500 nm. Analyses were performed using ANOVA with Tukey's post hoc test. The data are expressed as the mean ± standard deviation (SD). * $P < 0.05$ vs. sham group and # $P < 0.05$ vs. Mito group. ROSC, return of spontaneous circulation.

Figure 5. Mitochondrial transplantation reduces myocardial damage 4 hours after ROSC.

(A) Changes in superoxide dismutase activities and malondialdehyde levels in cardiac tissue (n = 7 animals per group). (B) Myocardial apoptosis levels were examined using TUNEL (n = 3 animals per group). Scale bar = 100 μm. (C) The percentage of myocardial apoptosis was examined using flow cytometry (n = 3 animals per group). (D) Quantitative analysis of myocardial TUNEL apoptosis index and flow apoptosis rate. (E) H&E staining was used to detect myocardial injury (n = 3 animals per group).

Scale bar = 100 μm. (F) The changes in CK-MB and cTn-I levels in the serum of rats were examined using ELISA (n = 7 animals per group). Analyses were performed using ANOVA with Tukey's post hoc test. The data were expressed as mean ± standard deviation (SD). * $P < 0.05$ vs. sham group and # $P < 0.05$ vs. Mito group. ROSC, return of spontaneous circulation; CK-MB, creatine kinase-MB fraction; cTn-I, cardiac troponin-I.

Figure 6. Potential mechanisms by which mitochondrial transplantation preserves cardiac function following ROSC.

Exogenous mitochondria enter the cell through actin-dependent endocytosis or macropinocytosis. A small number of mitochondria bind to lysosomes and are degraded. Most exogenous mitochondria can escape from the donor cells and play a role in recipient cells, altering the dynamic equilibrium of the receptor cells and exerting their protective function. ROSC, return of spontaneous circulation. By Figdraw.

Table 1 Baseline characteristics of rats and resuscitation characteristics ($\bar{x}$ ± s)

Variable	**n**	**Weight (g)**	**Temp (°C)**	**CA-induced time (sec)**	**CPR length (sec)**	**Adrenaline (mcg)**	**Pentobarbital sodium (mg)**
Sham	17	321.89±14.09	37.20±0.36	-	-	-	22.82±2.01
NS	17	318.65±10.00	37.45±0.43	234.29±22.89	128.41±12.50	12.75±0.40	21.63±1.35
Vehicle	17	326.80±11.64	37.33±0.37	247.06±23.61	138.82±14.64	13.07±0.47	21.79±0.98
Mito	17	320.64±14.32	37.45±0.39	241.29±23.38	131.88±14.51	12.83±0.57	21.92±1.05
***P*-Value**		0.29	0.21	0.57	0.10	0.13	0.07

n = 17 animals per group. CA, cardiac arrest; CPR, cardiopulmonary resuscitation.

All data are expressed as mean ± SE.

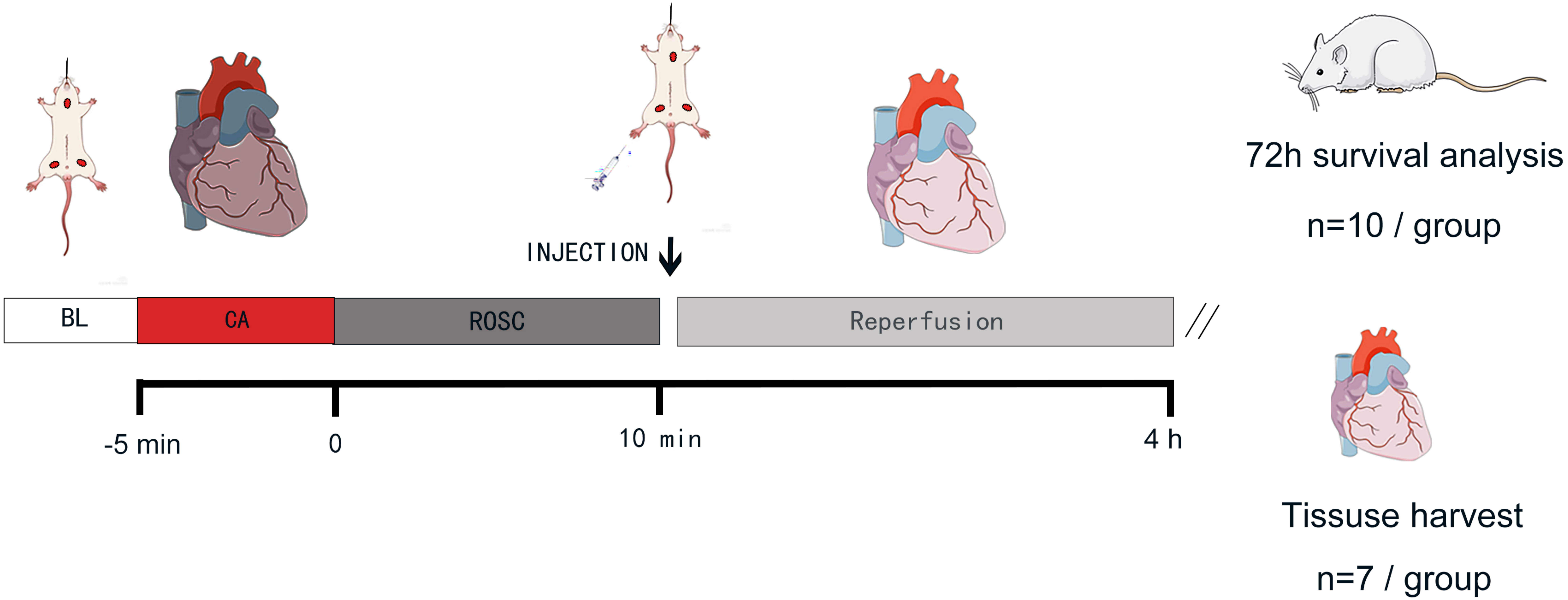
INJECTION
BL
CA
ROSC
Reperfusion
-5 min
0
10 min
4 h
72h survival analysis
n=10 / group
Tissuse harvest
n=7 / group

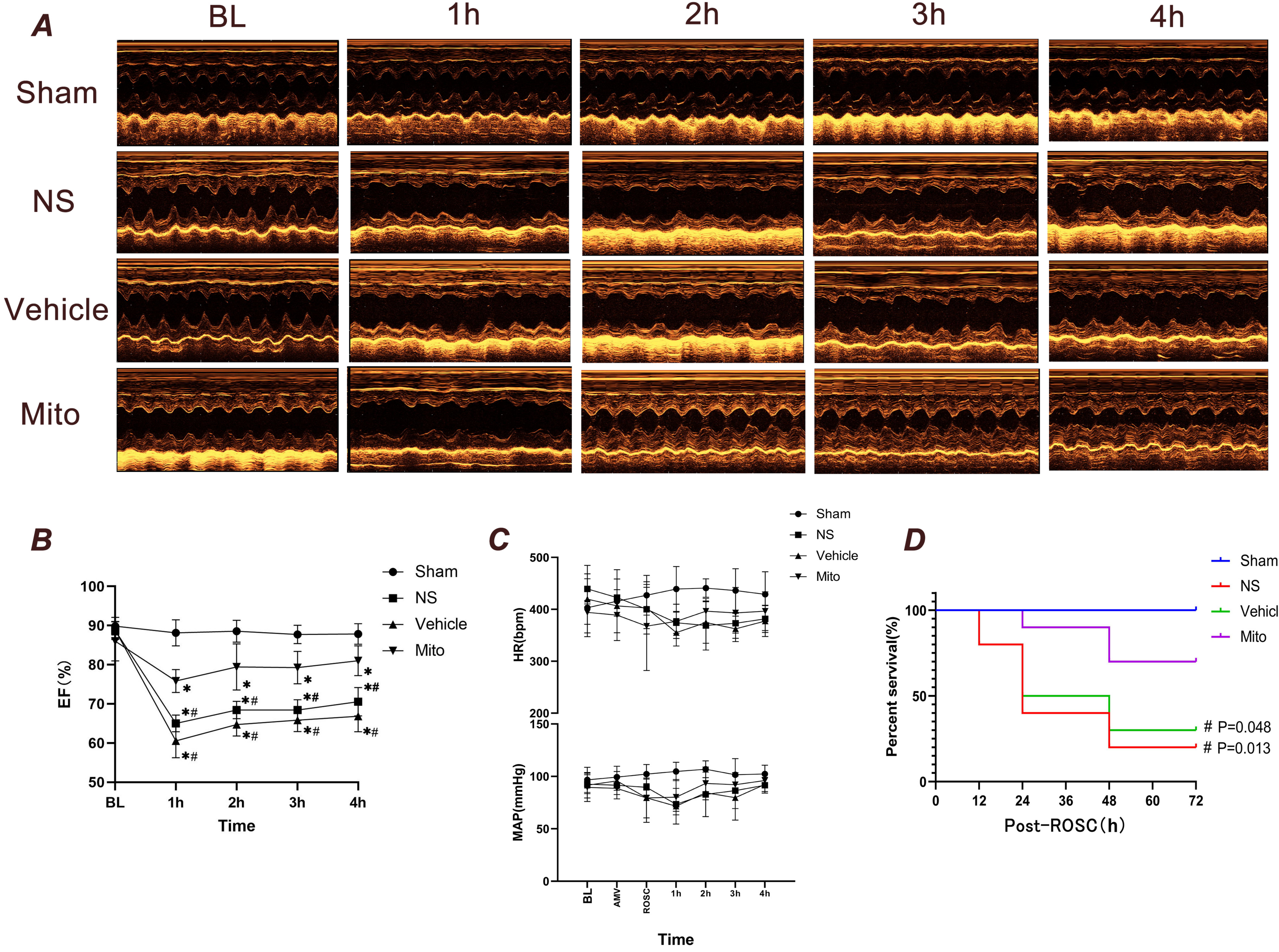
A
BL
1h
2h
3h
4h
Sham
NS
Vehicle
Mito
B
EF(%)
100
90
80
70
60
50
BL
1h
2h
3h
4h
Time
Sham
NS
Vehicle
Mito
*
*#
C
HR(bpm)
500
400
300
200
MAP(mmHg)
150
100
50
0
BL
AMV
ROSC
1h
2h
3h
4h
Time
Sham
NS
Vehicle
Mito
D
Percent servival(%)
100
50
0
0
12
24
36
48
60
72
Post-ROSC(h)
Sham
NS
Vehicle
Mito
# P=0.048
# P=0.013

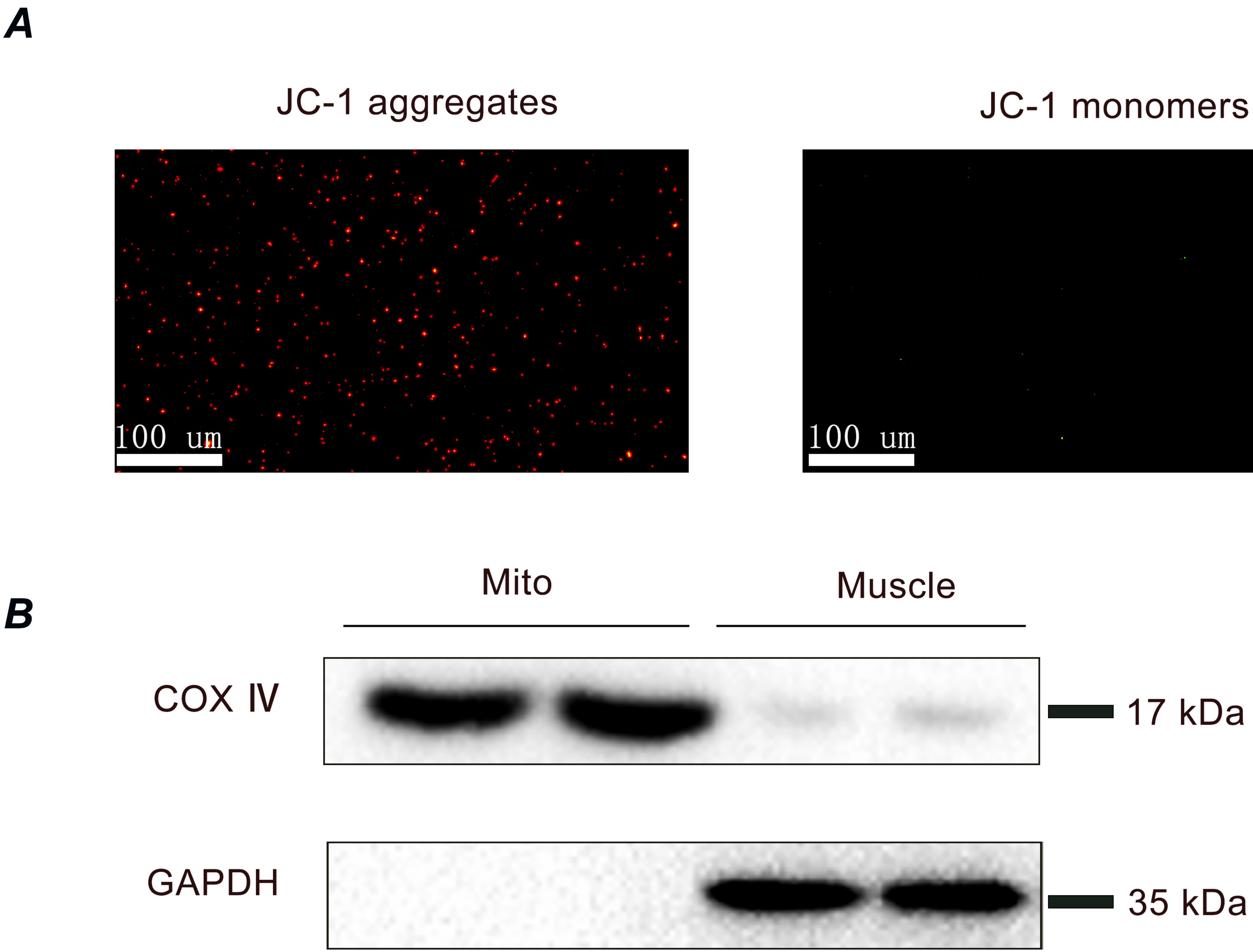
A
JC-1 aggregates
JC-1 monomers
100 um
100 um
B
Mito
Muscle
COX Ⅳ
17 kDa
GAPDH
35 kDa

A
DAPI
ACTN2
Mito-tracker
Merge
Sham
NS
Vehicle
Mito
100 um
3 um
B
complex Ⅱactivity（U/mg prot)
150
100
50
0
Sham
NS
Vehicle
Mito
*#
*#
*
C
complex Ⅳactivity（U/mg prot）
500
400
300
200
100
0
Sham
NS
Vehicle
Mito
*#
*#
*
D
ATP(umol/gprot)
150
100
50
0
Sham
NS
Vehicle
Mito
*#
*#
*
E
Fluorescence intensity of Tom20
80
60
40
20
0
Sham
NS
Vehicle
Mito
F
DAPI
Tom20
Merge
Sham
NS
Vehicle
Mito
100 um
G
Sham
NS
Vehicle
Mito
500 nm
500 nm
500 nm
500 nm

A
MDA (nmol/mgprot)
15
10
5
0
*#
*#
*
SOD (U/mgprot)
8
6
4
2
0
*#
*#
*
B
DAPI
TUNEL
MERGE
Sham
NS
Vehicle
Mito
100 um
C
PE-561-A
FITC-A
Sham
NS
Vehucle
Mito
D
Apoptosis indexes (%)
10
8
6
4
2
0
*#
*#
Sham
NS
Vehicle
Mito
apoptosis rate by Flow Cytometric Assay(%)
40
30
20
10
0
*#
*#
*
Sham
NS
Vehicle
Mito
E
100 um
Sham
NS
Vehicle
Mito
F
CK-MB (ng/ml)
40
30
20
10
0
*#
*#
*
Sham
NS
Vehicle
Mito
cTn-I(ng/L)
150
100
50
0
*#
*#
*
Sham
NS
Vehicle
Mito

Transplant mitochondria
Ischemia reperfusion
Myocardial function ↑
Aid
Damage
Fusion and fission
Lysosomal fusion
Autophagy
Dynamic equilibrium
CK-MB ↓
cTn-I ↓
Mitochondrial respiration ↑
ATP ↑
Apoptosis ↓
Oxidative stress ↓